Computer Assisted Mechanics and Engineering Sciences, 10: 177–199, 2003.


# Circular and annular two-phase plates of minimal compliance†

Krzysztof Kolanek
*Institute of Fundamental Technological Research, Polish Academy of Sciences*
*ul. Świętokrzyska 21, 00-049 Warsaw, Poland*

Tomasz Lewiński
*Warsaw University of Technology, Faculty of Civil Engineering*
*Institute of Structural Mechanics, Al. Armii Ludowej 16, 00-637 Warsaw, Poland*

(Received October 25, 2002)

The paper deals with optimal design of thin plates. The plate thickness assumes two possible values: $h_2$ and $h_1$ and the plate volume is given. The problem of minimizing the plate compliance needs relaxation. The relaxed formulation was found by Gibiansky and Cherkaev in 1984 [13]. In the present paper a finite element approximation of this problem is presented in the framework of rotationally symmetric bending of circular and annular plates.

The problem is composed of a nonlinear equilibrium problem coupled with a minimum compliance problem. The aim of the present paper is to analyze the forms of the optimal solutions, in particular, to look into the underlying microstructures. It is proved that in some solutions a ribbed microstructure occurs with ribs non-coinciding with both the radial and circumferential directions. Due to non-uniqueness of the sign of an angle of inclination of ribs the appearance of this microstructure does not contrasts with the radial symmetry of the problem. In the degenerated problem when the smallest thickness $h_1$ vanishes the above interpretation of the inclined ribbed microstructure becomes incorrect; in these regions one can assume that the plate is solid but with a varying thickness. The degenerated case of $h_1 = 0$ was considered in the papers by Rozvany et al. [26] and Ong et al. [25] but there such a microstructure was not taken into account. One of the aims of the paper is to re-examine these classical and frequently cited results.

## 1. Introduction

The subject of the paper is the following problem of optimization of thin two-phase plates: there is given an isotropic material of Young's modulus $E$ and Poisson ratio $\nu$. A plate made of such a material should occupy a plate domain, with a reference plane $\Omega$, assuming two possible thicknesses: $h_2$ and $h_1$, with $h_2 > h_1$, in the domains $\Omega_2$ and $\Omega_1$, respectively. The plate volume is fixed to be equal $V_0$. The plate is symmetric with respect to its middle plane $\Omega$. Let us assume for the time being that this plane is parametrized by a Cartesian coordinate system $(x_1, x_2)$ with the basis $(\mathbf{e}_1, \mathbf{e}_2)$. The plate is subjected to a transverse loading $q = q(x)$, $x = (x_1, x_2)$. The plate deflection $w$ is determined by the variational equilibrium equation:

$$\int_\Omega M^{\alpha\beta}\kappa_{\alpha\beta}(v)\mathrm{d}x = \int_\Omega qv\,\mathrm{d}x \qquad \forall v \in H(\Omega). \tag{1}$$

†This is an extended version of a paper presented at the conference *OPTY-2001, Mathematical and Engineering Aspects of Optimal Design of Materials and Structures*, Poznań, Poland, August 27–29, 2001.

Here, $H(\Omega)$ represents the space of kinematically admissible deflections $v$. The small Greek indices run over 1,2. Moreover,

$$M^{\alpha\beta} = D^{\alpha\beta\lambda\mu}\,\kappa_{\lambda\mu}(w), \qquad \kappa_{\lambda\mu}(w) = -\frac{\partial^2 w}{\partial x_\lambda \partial x_\mu}\,. \tag{2}$$

Tensor $\mathbf{D} = \left(D^{\alpha\beta\lambda\mu}\right)$ has the isotropic representation

$$\mathbf{D}(x) = 2k(x)\,\mathbf{I}_1 + 2\mu(x)\,\mathbf{I}_2 \tag{3}$$

where

$$k(x) = \frac{Eh^3(x)}{24(1-\nu)}\,, \qquad \mu(x) = \frac{Eh^3(x)}{24(1+\nu)}\,, \tag{4}$$

$$h(x) = \begin{cases} h_1 & \text{if } x \in \Omega_1\,, \\ h_2 & \text{if } x \in \Omega_2\,. \end{cases} \tag{5}$$

The tensors $\mathbf{I}_1$, $\mathbf{I}_2$ have the following components in the basis $\mathbf{e}_\alpha \otimes \mathbf{e}_\beta \otimes \mathbf{e}_\lambda \otimes \mathbf{e}_\mu$:

$$I_1^{\alpha\beta\lambda\mu} = \frac{1}{2}\delta^{\alpha\beta}\delta^{\lambda\mu}, \tag{6}$$

$$I_2^{\alpha\beta\lambda\mu} = \frac{1}{2}\left(\delta^{\alpha\lambda}\delta^{\beta\mu} + \delta^{\alpha\mu}\delta^{\lambda\beta}\right) - \frac{1}{2}\delta^{\alpha\beta}\delta^{\lambda\mu}. \tag{7}$$

The tensor of flexibilities $\mathbf{d} = \mathbf{D}^{-1}$ has the following representation,

$$\mathbf{d}(x) = 2K(x)\,\mathbf{I}_1 + 2L(x)\,\mathbf{I}_2\,, \tag{8}$$

where

$$K = 1/k, \qquad L = 1/\mu. \tag{9}$$

According to Eq. (5) the functions $K(x)$, $L(x)$, $k(x)$, $\mu(x)$ are determined by the quantities

$$K_\alpha = 1/k_\alpha\,, \qquad L_\alpha = 1/\mu_\alpha\,, \qquad k_\alpha = \frac{E(h_\alpha)^3}{24(1-\nu)}\,, \qquad \mu_\alpha = \frac{E(h_\alpha)^3}{24(1+\nu)}\,. \tag{10}$$

The compliance of the plate, defined by the formula

$$C = \int_\Omega qw\,\mathrm{d}x, \tag{11}$$

is determined by the division of the domain $\Omega$ into the subdomains $\Omega_\alpha$, where $h = h_\alpha$. Let us remind that the plate volume is fixed,

$$\int_\Omega h(x)\,\mathrm{d}x = V_0 \tag{12}$$

or

$$h_1\,|\Omega_1| + h_2\,|\Omega_2| = V_0\,, \tag{13}$$

where $|\Omega_\alpha|$ means the area of the domain $\Omega_\alpha$.

The classical problem of optimum design of elastic two-phase plates is formulated as follows. Given are: $\Omega$, the boundary conditions, $h_2$, $h_1$, $E$, $q$, $\nu$. The problem reads:

| minimize $C$ under the condition of the volume being fixed by Eq. (12);<br>the function $w$ entering Eq. (11) satisfies Eqs. (1)-(2) with $\mathbf{D}$ given by Eqs. (3)-(5) | $(P_0)$ |
|---|---|

The problem above is ill posed in the sense that in general it admits no solution. Furthermore, the possible solution is not stable with respect to the small perturbations of the data of the problem. Moreover, this phenomenon is confirmed by numerical experiments. Such a behaviour of the problem $(P_0)$ is not exceptional, similar phenomena are observed in many layout optimization problems, see Cherkaev [9]. Thus the problem $(P_0)$ necessitates a reformulation; in the mathematical literature such a reformulation is called relaxation. The history of discovering of relaxation by homogenization has recently been written by L. Tartar [28]. The ideas of Tartar were inspiration of the subsequent papers in which the question of formulation of the relaxation setting for the layout optimization of plane elasticity and for the Kirchhoff plates bending problem was effectively solved, see Gibiansky and Cherkaev [13], Lurie and Cherkaev [23], Kohn and Strang [16] and Allaire and Kohn [1, 2]. The relaxation of the problem $(P_0)$ was for the first time discovered by Gibiansky and Cherkaev [13]. There the formulation was based upon the complementary energy principle and the final setting involved moments as unknowns. This setting has been transformed to the displacement-based formulation by Lewiński and Telega [19, Sec. 26.6]. This formulation will be recalled in the next section. Let us note that in papers by Rozvany et al. [26] and Ong et al. [25] the authors considered similar problems in the case of circular one-phase plates under rotationally symmetric loadings; the case of one phase means that $h_1 = 0$. The authors of [25, 26], inspired by the paper of Kohn and Strang [16] concerning the optimization problems within linear elasticity, assumed that the optimal plates have a ribbed 2nd rank microstructure with ribs lying along the radial and circumferential directions. This means that then these directions coincide with directions of principal moments and curvatures. In the case of two-phase layout problems of plane elasticity one can prove rigorously that this is just the case: the ribbed (or laminated) microstructure should coincide with principal directions of stress and strain tensors. In the case of two-phase thin plates (when $h_1 > 0$) the optimal microstructure behaves differently; there are domains (to be specified rigorously in the next section) where the inclination of ribs deviate from the principal directions of moments. On the other hand, these latter directions always coincide with principal directions of strains, see Gibiansky and Cherkaev [13] and Lewiński and Telega [19]. This deviation can occur also in the rotationally symmetric solutions, which does not contradict this symmetry. One should remind that the sign of the angle of deviation is undefined and two directions of ribs are simultaneously possible, as schematically outlined in Fig. 1. One can imagine that the ribs are alternately directed along the radial direction of a circular plate, which retrieves symmetry of the optimal solution. In the case of $h_1 = 0$ the interpretation of Fig. 1 loses its sense, since such microstructure becomes unstable, but instead the optimal microstructure must have isotropic properties.

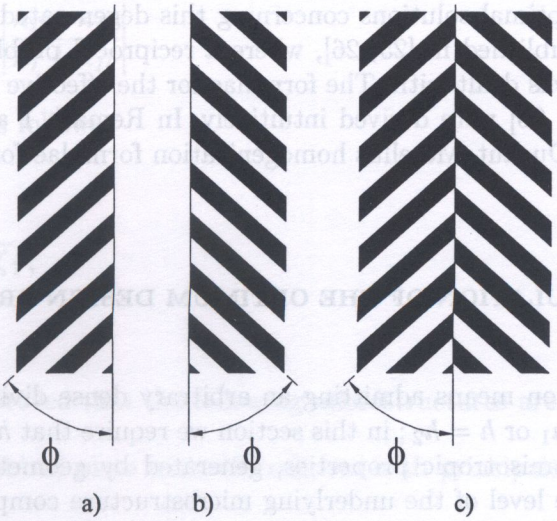


**Fig. 1.** An oblique microstructure predicted by Gibiansky and Cherkaev [13]; a,b) – possible inclinations of ribs, c) – treelike microstructure composed of alternate oblique ribs

Thus the analytical and numerical solutions found in [25, 26] have been found under additional constraints imposed on the optimal microstructure of Gibiansky and Cherkaev. One of the conclusions of papers [25, 26] is that the 2nd rank microstructure does not appear. It is possible that this is the consequence of the mentioned microstructural constraints. The optimal solutions found in the present paper do involve the 2nd rank ribbed microstructure as well as the first rank oblique microstructure with ribs deviating from the principal directions of moments.

The papers of Gibiansky Cherkaev [13], Lurie Cherkaev [23], Allaire and Kohn [1, 2] were based upon the earlier works of Kozłowski and Mróz [18], Cheng [6] and Cheng and Olhoff [7, 8], Olhoff et al. [24], Rozvany et al. [27]. These papers played an important role and for sure helped Gibiansky and Cherkaev and Allaire and Kohn to find a correct and final relaxed formulation. In the present paper we shall not compare our results with those published in [6–8, 18, 24, 27] because of the following reasons. In [18] different merit functions have been analyzed. In [6–8, 24] different ranges of variation of $h(x)$ were considered, e.g. the case where $h_1 \leq h(x) \leq h_2$. Nowhere the oblique microstructure was considered; its existence lies beyond a sound imagination and can be viewed as a paradox linked with the Kirchhoff assumption of constraint rotations.

The optimum design of plates has also been considered by the following methods: the bubble method of Eschenauer et al. [12], the evolutionary methods developed by Liang et al. [21], the SIMP approach in the version of Belblidia et al. [3]. The mentioned methods give suboptimal solutions, since they do not represent any approximation to the correct relaxed formulation of Gibiansky and Cherkaev [13]. Thus any comparisons with the results of the papers mentioned would be irrelevant. The role of the mentioned approaches lies in making the optimal (in fact, suboptimal) solutions closer to those expected by designers, at least to the really manufactured forms, see Bendsøe [4] and Bendsøe and Sigmund [5].

The paper is organized as follows. In Section 2 the relaxed formulation in its displacement-based form is recalled after [19, Sec. 26], cf. Lipton [22] and Telega and Lewiński [29]. This formulation leads to a saddle point formulation $(P)$.

In Section 4 we give an outline of the numerical algorithm of solving this problem. The nonlinear equilibrium problems are solved by the FEM targeted at hyperelasticity, see Kleiber [15]. In Section 5 we present an analysis of optimal solutions of selected problems . There are considered: the clamped circular plates under a uniform transverse loading, the same plates, but simply supported, and annular plates supported along the outer edge. The method of finding these solutions was announced by Kolanek and Lewiński [17].

The case of shape design or $h_1 = 0$ requires a special caution. The relaxed formulation still holds but the hyperelastic potential loses its smoothness, see [19, Sec. 26.7] and [20]. In Section 5 we consider a sequence of optimal solutions concerning this degenerated case. These solutions can be confronted with those published in [25, 26], where a reciprocal problem (minimize the volume under a given compliance) was dealt with. The formulae for the effective stiffnesses of ribbed plates of second rank given in [25, 26] were derived intuitively. In Remark 1 a proof is given that these formulae coincide with the Duvaut–Metellus homogenization formulae for thin plates, as derived in Section 24.2 of [19].

## 2. The relaxed formulation of the optimum design problem $(P_0)$. Case of $h_1 > 0$

Relaxation by homogenization means admitting an arbitrary dense division of the domain $\Omega$ into the subdomains where $h = h_1$ or $h = h_2$; in this section we require that $h_2 > h_1 > 0$. Consequently, the optimal plate assumes anisotropic properties, generated by geometry of the domains, where $h = h_1$ or $h = h_2$ but at the level of the underlying microstructure composed of repetitive cells $Y$. Within these cells the area fraction of the phase, where $h = h_2$ is equal to $m_2$ and this fraction represents one of the design variables of the problem. It turns out that the effective plate endowed with the microstructure of Gibiansky–Cherkaev has hyperelastic properties, the relevant constitutive

equation being given by [19, Eq. 26.6.7],

$$\mathbf{M} = \frac{\partial W(\boldsymbol{\kappa}, m_2)}{\partial \boldsymbol{\kappa}}, \tag{14}$$

where $W$ represents the hyperelastic potential. In order to define the potential $W(\boldsymbol{\kappa}, m_2)$ we introduce the following notation. The invariants of the tensor $\boldsymbol{\kappa}$ are defined by

$$I(\boldsymbol{\kappa}) = \frac{1}{\sqrt{2}} \operatorname{tr} \boldsymbol{\kappa}, \qquad II(\boldsymbol{\kappa}) = \frac{1}{\sqrt{2}} \left[ (\operatorname{tr} \boldsymbol{\kappa})^2 - 4 \det \boldsymbol{\kappa} \right]^{1/2}. \tag{15}$$

They can be put in the form

$$I(\boldsymbol{\kappa}) = \frac{1}{\sqrt{2}} (\kappa_I + \kappa_{II}), \qquad II(\boldsymbol{\kappa}) = \frac{1}{\sqrt{2}} |\kappa_I - \kappa_{II}|, \tag{16}$$

where $\kappa_I$, $\kappa_{II}$ are principal values of the tensor $\boldsymbol{\kappa}$. Let us introduce the auxiliary quantities

$$\Delta k = k_2 - k_1, \qquad \Delta \mu = \mu_2 - \mu_1, \qquad m_1 = 1 - m_2, \tag{17}$$

$$\begin{aligned} [k]_m &= m_1 k_2 + m_2 k_1, & [\mu]_m &= m_1 \mu_2 + m_2 \mu_1, \\ \langle k \rangle_m &= m_1 k_1 + m_2 k_2, & \langle \mu \rangle_m &= m_1 \mu_1 + m_2 \mu_2, \end{aligned} \tag{18}$$

$$\breve{\zeta}_1 = \frac{\Delta k}{\Delta \mu}, \qquad \breve{\zeta}_2 = \frac{m_2 \Delta k}{\mu_2 + [k]_m}, \tag{19}$$

$$\begin{aligned} \breve{a}_1 &= \langle k \rangle_m, & \breve{a}_2 &= \frac{k_1 k_2 + \mu_2 \langle k \rangle_m}{\mu_2 + [k]_m}, \\ \breve{c}_1 &= \langle \mu \rangle_m, & \breve{c}_2 &= \mu_2 \\ \breve{A}_1 &= \frac{m_1 m_2 (\Delta \mu)^2}{[k]_m + [\mu]_m}, & \breve{A}_2 &= \frac{m_1 \Delta \mu (\mu_2 + [k]_m)}{[k]_m + [\mu]_m}. \end{aligned} \tag{20}$$

It turns out that the plate domain is divided into three domains determining so called regimes of the solution. They are controlled by the value of the following scalar invariant of the strain tensor

$$\zeta_\kappa = \frac{II(\boldsymbol{\kappa})}{|I(\boldsymbol{\kappa})|}, \qquad \zeta_\kappa = \left| \frac{\kappa_I - \kappa_{II}}{\kappa_I + \kappa_{II}} \right|. \tag{21}$$

The regimes are defined as follows:

(i) regime 3: $\zeta_\kappa \le \breve{\zeta}_2$,

(ii) regime 2: $\breve{\zeta}_2 \le \zeta_\kappa \le \breve{\zeta}_1$,

(iii) regime 1: $\zeta_\kappa \ge \breve{\zeta}_1$.

Gibiansky and Cherkaev proved that the following microstructures are realized in the regimes 1–3:

(i) regime 3: 2nd rank ribbed plate with ribs colinear with principal directions of $\boldsymbol{\kappa}$,

(ii) regime 2: 1st rank ribbed plate with ribs colinear with principal directions of $\boldsymbol{\kappa}$,

(iii) regime 1: 1st rank ribbed plate with ribs non-colinear with principal directions of $\boldsymbol{\kappa}$.

The complete characterization of these microstructures are given in Section 26 of [19]. Let us define the auxiliary functions

$$F_\alpha(x) = \breve{a}_\alpha + \breve{c}_\alpha x^2 , \tag{22}$$

$$\widetilde{F}(x) = F_1(x) - \breve{A}_1\left(x - \breve{\zeta}_1\right)^2 = F_2(x) - \breve{A}_2\left(x - \breve{\zeta}_2\right)^2 . \tag{23}$$

The last equality holds due to identities

$$\breve{a}_1 - \breve{A}_1(\breve{\zeta}_1)^2 = \breve{a}_2 - \breve{A}_2(\breve{\zeta}_2)^2 , \qquad \breve{A}_2\breve{\zeta}_2 = \breve{A}_1\breve{\zeta}_1 , \qquad \breve{c}_1 - \breve{A}_1 = \breve{c}_2 - \breve{A}_2 , \tag{24}$$

which can be proved by inspection. We see that the parabola $\widetilde{F}(x)$ is tangent to the parabola $F_1(x)$ at $x = \breve{\zeta}_1$ and tangent to the parabola $F_2(x)$ at $x = \breve{\zeta}_2$. Moreover, $\widetilde{F}(x)$ lies below the parabolas $F_1(x)$, $F_2(x)$. Now we are ready to define the potential $W$,

$$W(\boldsymbol{\kappa}, m_2) = \begin{cases} [I(\boldsymbol{\kappa})]^2 F(\zeta_\kappa) & \text{if } I(\boldsymbol{\kappa}) \neq 0, \\ \langle \mu \rangle_m [II(\boldsymbol{\kappa})]^2 & \text{if } I(\boldsymbol{\kappa}) = 0, \end{cases} \tag{25}$$

where the function $F$ is defined by stitching the parabolas $F_1(x)$, $\widetilde{F}(x)$, $F_2(x)$ as follows

$$F(x) = \begin{cases} F_2(x) & \text{if } x \in \left[0, \breve{\zeta}_2\right], \\ \widetilde{F}(x) & \text{if } x \in \left[\breve{\zeta}_2, \breve{\zeta}_1\right], \\ F_1(x) & \text{if } x \geq \breve{\zeta}_1 . \end{cases} \tag{26}$$

Differentiation in Eq. (14) can be performed explicitly. It gives the constitutive relation in the following alternative form

$$M^{\alpha\beta} = D^{\alpha\beta\lambda\mu}(\boldsymbol{\kappa}, m_2)\, \kappa_{\lambda\mu}(w) \tag{27}$$

with

$$\mathbf{D}(\boldsymbol{\kappa}, m_2) = 2k(\boldsymbol{\kappa}, m_2)\, \mathbf{I}_1 + 2\mu(\boldsymbol{\kappa}, m_2)\, \mathbf{I}_2 . \tag{28}$$

The functions $k(\boldsymbol{\kappa}, m_2)$, $\mu(\boldsymbol{\kappa}, m_2)$ are defined as follows, cf. [17]. If $I(\boldsymbol{\kappa}) = 0$ we have

$$k(\boldsymbol{\kappa}, m_2) = 0, \qquad \mu(\boldsymbol{\kappa}, m_2) = \langle \mu \rangle_m . \tag{29}$$

Otherwise, i.e. for $I(\boldsymbol{\kappa}) \neq 0$, one finds

$$k(\boldsymbol{\kappa}, m_2) = \begin{cases} \breve{a}_2 & \text{if } \zeta_\kappa \in \left[0, \breve{\zeta}_2\right], \\ \breve{a}_\alpha - \breve{A}_\alpha \breve{\zeta}_\alpha \left(\breve{\zeta}_\alpha - \zeta_\kappa\right) & \text{if } \zeta_\kappa \in \left[\breve{\zeta}_2, \breve{\zeta}_1\right], \\ \breve{a}_1 & \text{if } \zeta_\kappa \geq \breve{\zeta}_1 , \end{cases} \tag{30}$$

$$\mu(\boldsymbol{\kappa}, m_2) = \begin{cases} \breve{c}_2 & \text{if } \zeta_\kappa \in \left[0, \breve{\zeta}_2\right], \\ \breve{c}_\alpha - \breve{A}_\alpha \left(1 - \breve{\zeta}_\alpha / \zeta_\kappa\right) & \text{if } \zeta_\kappa \in \left[\breve{\zeta}_2, \breve{\zeta}_1\right], \\ \breve{c}_1 & \text{if } \zeta_\kappa \geq \breve{\zeta}_1 . \end{cases} \tag{31}$$

By virtue of the identities (24) the expressions depending on $\alpha$ assume the same values for $\alpha = 1$ and $\alpha = 2$.

The equilibrium problem of an effective hyperelastic plate has the form of the maximization problem

$$C(m_2) = \max_{v \in H(\Omega)} \int_\Omega (2qv - 2W(\boldsymbol{\kappa}(v), m_2)) \, \mathrm{d}x \tag{32}$$

Here $C(m_2)$ represents the plate compliance. The area fraction of the plate material determined by the thickness $h = h_2$ equals $m_2(x)$. Thus the plate thickness is represented by the integral of the expression $h_1 m_1(x) + h_2 m_2(x)$, where $m_1(x) = 1 - m_2(x)$. The isoperimetric condition (12) is replaced with the condition expressed in terms of $m_2(x)$,

$$\int_\Omega (h_1 m_1(x) + h_2 m_2(x)) \, \mathrm{d}x = V_0 \tag{33a}$$

or

$$\int_\Omega m_2(x) \, \mathrm{d}x = A_0 \,, \tag{33b}$$

where

$$A_0 = \frac{V_0 - h_1 |\Omega|}{(h_2 - h_1)}$$

and $|\Omega|$ represents the area of $\Omega$.

The relaxed problem corresponding to the problem $(P_0)$ has the form, see [19, Sec. 26],

$$\min \{C(m_2) \mid m_2 \in L^\infty(\Omega, [0,1]) \text{ and the condition (33b) holds}\} \tag{$P$}$$

The problem $(P)$ consists in finding the saddle point of the functional

$$J(v) = 2 \int_\Omega (qv - W(\boldsymbol{\kappa}(v), m_2)) \, \mathrm{d}x \tag{34}$$

with respect to the fields $v(x)$ and $m_2(x)$. This saddle point exists, see Lipton [22], Lewiński and Telega [19, Sec. 26.6] and Telega and Lewiński [29]. The solution to the problem $(P)$ is the pair $(w, m_2)$ that determines three regimes: 1,2 and 3. These regimes are realized in certain domains and just finding their shapes is one of the aims of the project. In particular, we are interested in finding the boundaries between these domains, where

$\zeta_\kappa = \breve{\zeta}_1$ (the boundary between the domains corresponding to the regimes 1 and 2),

$\zeta_\kappa = \breve{\zeta}_2$ (the boundary between the domains corresponding to the regimes 2 and 3).

Let us remind that $m_2 = 0$ means $h = h_1$ and the case of $m_2 = 1$ refers to the case of $h = h_2$.

In the regime 2 the microstructure is that of a first rank ribbed plate and $m_2(x)$ represents the area fraction of the 2nd phase or $h = h_2$. In this regime the ribs lie along the trajectories of the principal moments.

In the regime 3 the microstructure is that of 2nd rank ribbed *plate material* with ribs direction coinciding with trajectories of the principal moments. The vector $\mathbf{e}_1$ in Fig. 2 can be directed along the first or second principal moment, hence two possible microstructures realize the optimum solution and correspond to that expression for the potential $W$ which refers to the case of regime 3. The area fraction $\theta_1$ is determined by the formula

$$\theta_1 = \frac{1}{2}\left(1 + m_1 \pm \frac{m_2}{\zeta_2} \frac{II(\mathbf{M})}{I(\mathbf{M})}\right) \tag{35}$$

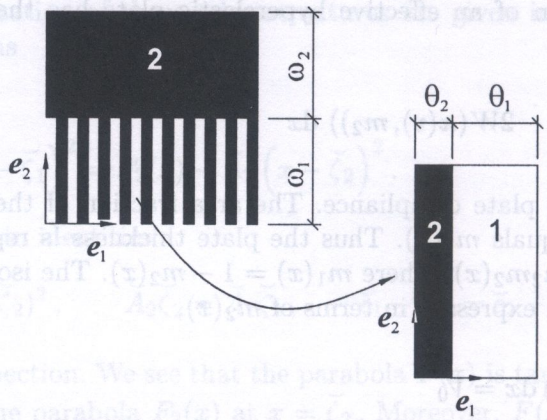


**Fig. 2.** Ribbed microstructure of 2nd rank. The first homogenization of both the phases is performed along versor $\mathbf{e}_1$ with area fractions $\theta_1$, $\theta_2$. The second homogenization concerns the previous material and the stronger phase 2 along the versor $\mathbf{e}_2$ with area fractions $\omega_1$, $\omega_2$. Thus the weaker phase is a core and the stronger phase is an envelope

where

$$\zeta_2 = \frac{m_2 \Delta k}{\frac{k_1 k_2}{\mu_2} + \langle k \rangle_m} \tag{36}$$

and $I(\mathbf{M})$ and $II(\mathbf{M})$ are defined as in Eq. (15). The sign + in Eq. (35) refers to the case of $\mathbf{e}_1$ being directed along the first principal direction of $\mathbf{M}$. The sign − refers to the case of the second principal direction of $\mathbf{M}$.

In the domain of regime 1 the ribbed microstructure is of 1st rank of direction $\mathbf{e}_1$ deviated by angle $\phi$ from the first principal direction of $\mathbf{M}$, see Fig. 1. The quantity $\cos 2\phi$ is determined uniquely,

$$\cos 2\phi = -\frac{I(\mathbf{M})}{II(\mathbf{M})}\,\zeta_1\,, \tag{37}$$

where

$$\zeta_1 = \frac{\langle \mu \rangle_m}{\langle k \rangle_m}\,\frac{\Delta k}{\Delta \mu}\,. \tag{38}$$

Appearance of such microstructure does not contradict principles of symmetry since the sign of the angle $\phi$ is undefined, cf. Fig. 1. The sole knowledge of the distribution of $\boldsymbol{\kappa}$ and $m_2$ in the domain $\Omega$ suffices to fix the type and characteristics of feasible microstructures in all the regimes.

## 3. The relaxed formulation of the shape design problem

The case of $h_1 = 0$ refers to the shape design. Then $h$ assumes only the value $h_2$. In the formulation $(P_0)$ the domain $\Omega$ is divided into two regions: a solid region $\Omega_2$ and the holes $\Omega_1$. The relaxed formulation $(P)$ admits additional regions with a perforated microstructure. The formal substitution: $k_1 = 0$, $\mu_1 = 0$ into Eq. (25) gives, see [19, 20],

$$W(\boldsymbol{\kappa}, m_2) = \begin{cases} [I(\boldsymbol{\kappa})]^2 F_0(\zeta_\kappa) & \text{if } I(\boldsymbol{\kappa}) \neq 0, \\ m_2 \mu_2 [II(\boldsymbol{\kappa})]^2 & \text{if } I(\boldsymbol{\kappa}) = 0. \end{cases} \tag{39}$$

Let us define the counterparts of $\breve{\zeta}_1$, $\breve{\zeta}_2$,

$$\breve{\zeta}_1^0 = \frac{k_2}{\mu_2}\,, \qquad \breve{\zeta}_2^0 = \frac{m_2 k_2}{\mu_2 + m_1 k_2}\,, \tag{40}$$

and the counterpart of $F$, see Eq. (26)

$$F_0(x) = \begin{cases} \mu_2 \left( \breve{\zeta}_2^0 + x^2 \right) & \text{if } x \in \left[ 0, \breve{\zeta}_2^0 \right], \\ \dfrac{m_2 k_2 \mu_2}{k_2 + \mu_2} (1+x)^2 & \text{if } x \in \left[ \breve{\zeta}_2^0, \breve{\zeta}_1^0 \right], \\ m_2 \mu_2 \left( \breve{\zeta}_1^0 + x^2 \right) & \text{if } x \geq \breve{\zeta}_1^0. \end{cases} \tag{41}$$

One can prove that the case of $\breve{\zeta}_2{}^0 \leq \zeta_\kappa \leq \breve{\zeta}_1^0$ corresponds to the case of $\zeta_M = 1$, which means $\det \mathbf{M} = 0$ or $M_I M_{II} = 0$. Thus in the sliding regime 2 one of the principal moments vanishes.

Since the case of $h_1 = 0$ introduces some degenerations the question arises whether the microstructures described in Section 2 characteristic for the regimes 1–3 realize the relaxed potential (39). Consider the regimes in Eq. (41).

***Regime 3.*** $\zeta_\kappa \leq \breve{\zeta}_2^0$

In the case of $h_1 \neq 0$ the proof of attainability of the potential on the 2nd rank non-rotated microstructure is based on Lemma 24.1 of [19]. In the case of $h_1 = 0$ the formulae for the non-vanishing flexibilities $d_{\beta\alpha}^{0hh}$ of the 2nd rank microstructure of Fig. 2, given by Eqs. (24.2.8) in [19], reduce to the form

$$2d_{11}^{0hh} = K_2 + \frac{m_1 m_2 (K_2 + L_2)}{4\theta_2(\theta_1 - m_1)}, \qquad 2d_{22}^{0hh} = L_2 + \frac{m_1 m_2 (K_2 + L_2)}{4\theta_2(\theta_1 - m_1)},$$
$$2d_{12}^{0hh} = -\frac{m_1(2\theta_1 - 1 - m_1)(K_2 + L_2)}{4\theta_2(\theta_1 - m_1)}, \qquad 2d_{33}^{0hh} = \frac{L_2}{m_2}, \tag{42}$$

where

$$m_1 = \theta_1 \omega_1, \qquad \theta_2 = 1 - \theta_1, \qquad \{L\}_m = \left( \frac{m_1}{L_1} + \frac{m_2}{L_2} \right)^{-1},$$

cf. Eq.(10). Let us consider the function

$$H(\theta_1; x, y) = 2 \left[ d_{11}^{0hh}(\theta_1) x^2 + 2 d_{12}^{0hh}(\theta_1) xy + d_{22}^{0hh}(\theta_1) y^2 \right] \tag{43}$$

The counterpart of the Lemma 24.1 of [19] for the case of $h_1 = 0$ reads

**Lemma 1.** *Assume that $x \neq 0$, $y \neq 0$ and $|y/x| \leq 1$. Then*

$$\min_{0 \leq \theta_1 \leq 1} H(\theta_1; x, y) = H(\theta_1^*; x, y) \tag{44}$$

*where*

$$\theta_1^* = \frac{1}{2} \left( 1 + m_1 + m_2 \frac{y}{x} \right) \tag{45}$$

*and*

$$H(\theta_1^*; x, y) = K^0 x^2 + L_2 y^2, \qquad K^0 = \frac{K_2 + L_2 m_1}{m_2}. \tag{46}$$

**Proof.** Differentiation of the function $H(\theta_1; x, y)$ with respect to $\theta_1$ and equating this expression to zero gives two roots. The first one is given by Eq. (45) and the second one equals

$$\theta_1^{**} = \frac{1}{2} \left( 1 + m_1 + m_2 \frac{x}{y} \right).$$

This first root realizes the minimum of the function $H$. The substitution $\theta_1 = \theta_1^*$ gives the mentioned result (46). Thus in the regime 3 the 2nd rank microstructure is realized, see Fig. 2, with ribs lying along the trajectories of principal moments. □

***Regime 2.*** $\breve{\zeta}_2^0 \leq \zeta_\kappa \leq \breve{\zeta}_1^0$

Let us compute the stiffnesses $D_h^{0\alpha\beta}$ of the first rank ribbed plate with area fractions $m_1$, $m_2$, according to Eqs. (24.2.7) in [19]. By putting $\omega_\alpha = m_\alpha$ and $k_1 = \mu_1 = 0$ we find

$$D_h^{011} = D_h^{012} = D_h^{022} = \frac{2k_2\,\mu_2\,m_2}{k_2 + \mu_2} \tag{47}$$

which gives

$$D_h^{011}x^2 + 2D_h^{012}xy + D_h^{022}y^2 = \frac{2k_2\,\mu_2\,m_2}{k_2 + \mu_2}(x+y)^2. \tag{48}$$

By putting $x = I(\boldsymbol{\kappa})$, $y = II(\boldsymbol{\kappa})$, we confirm the result (39)–(41) in the case of $I(\boldsymbol{\kappa}) \neq 0$ and a given range of $\zeta_\kappa$.

***Regime 1.*** $\zeta_\kappa \geq \breve{\zeta}_1^0$

According to Eq. (39) the potential $W$ assumes the form

$$W(\boldsymbol{\kappa}, m_2) = \frac{1}{2}m_2\left(2k_2[I(\boldsymbol{\kappa})]^2 + 2\mu_2[II(\boldsymbol{\kappa})]^2\right) \tag{49}$$

while its reciprocal form reads, see Section 26.7 in [19],

$$W^*(\mathbf{M}, m_2) = \frac{1}{4m_2}\left(K_2[I(\mathbf{M})]^2 + L_2[II(\mathbf{M})]^2\right). \tag{50}$$

One can write

$$m_2k_2 = \frac{Eh_m^3}{24(1-\nu)}, \qquad m_2\mu_2 = \frac{Eh_m^3}{24(1+\nu)}, \qquad h_m^3 = m_2(h_2)^3. \tag{51}$$

Thus in this regime $W$ corresponds to a solid plate of varying thickness $h_m = \sqrt[3]{m_2}h_2$.

Note that this interpretation contradicts the initial assumption of $h$ assuming only two values (here 0 and $h_2$). The oblique first rank microstructure cannot be invoked here, in the case considered it ceases to be stable.

***Remark 1***

Let us compute the effective flexibilities $d_{\alpha\beta\lambda\mu}^{0hh}$ referred to the basis $\mathbf{e}_\alpha \otimes \mathbf{e}_\beta \otimes \mathbf{e}_\lambda \otimes \mathbf{e}_\mu$. By inverting the relations (21.1.24) of [19]) one finds

$$\begin{aligned} d_{1111}^{0hh} &= \frac{1}{2}\left(d_{11}^{0hh} + d_{22}^{0hh} + 2d_{12}^{0hh}\right), & d_{1122}^{0hh} &= \frac{1}{2}\left(d_{11}^{0hh} - d_{22}^{0hh}\right), \\ d_{2222}^{0hh} &= \frac{1}{2}\left(d_{11}^{0hh} + d_{22}^{0hh} - 2d_{12}^{0hh}\right), & d_{1212}^{0hh} &= \frac{1}{2}d_{33}^{0hh}. \end{aligned} \tag{52}$$

Let us note that $K_2 + L_2 = \frac{4}{EJ}$, with $J = \frac{(h_2)^3}{12}$. Substitution of Eq. (42) gives

$$\begin{aligned} d_{1111}^{0hh} &= \frac{1}{\omega_2}\frac{1}{EJ}, & d_{1122}^{0hh} &= -\frac{\nu}{EJ}, \\ d_{2222}^{0hh} &= \frac{1-\omega_2+\theta_2\omega_2}{\theta_2}\frac{1}{EJ}, & d_{1212}^{0hh} &= \frac{1+\nu}{2EJ}\frac{1}{\omega_2+\theta_2-\omega_2\theta_2}. \end{aligned} \tag{53}$$

The formulae above coincide with the formulae derived in [25, 26], where the following notation is used: $d_1 = \omega_2$, $d_2 = \theta_2$. Let us add that the formula for $d_{1111}^{0hh}$ ceases to be correct if $\theta_2 = 1$. Then we have $d_{1111}^{0hh} = 1/EJ$. Thus the operations: $\lim_{\theta_2 \to 1}$ and $\lim_{K_1 \to \infty, L_1 \to \infty}$ do not commute. Note that $d_{1122}^{0hh}$ does not depend on $\theta_2$, $\omega_2$ and vanishes for $\nu = 0$. Moreover, the flexibilities $d_{1111}^{0hh}$, $d_{2222}^{0hh}$ do not depend on the Poisson ratio.

## 4. Numerical procedure

Let us define the Lagrangian function for the problem $(P)$,

$$\mathcal{L} = \int_\Omega \left[2qv - 2W(\boldsymbol{\kappa}(v), m_2) + \lambda m_2 + \lambda_1(-m_2 + \alpha_1^2) + \lambda_2(-1 + m_2 + \alpha_2^2)\right] \mathrm{d}x, \tag{54}$$

where $\lambda$, $\lambda_1$, $\lambda_2$ are multipliers for the conditions (33b), $m_2 \geq 0$, $m_2 \leq 1$, respectively. The numbers $\alpha_1$, $\alpha_2$ are slack variables. The stationary condition $\delta\mathcal{L} = 0$ with respect to $v$, $m_2$, $\lambda$, $\lambda_1$, $\lambda_2$ gives, in particular,

$$-2\frac{\partial W}{\partial m_2} + \lambda + \lambda_2 - \lambda_1 = 0. \tag{55}$$

Let us define the function

$$Q(m_2, \lambda) = \frac{2}{\lambda}\frac{\partial W}{\partial m_2}. \tag{56}$$

A numerical solution to $(P)$ is found iteratively. The following formula for updating the design function $m_2$ was proposed by Olhoff et al. [24, Eq. (5.9)] and Bendsøe [4],

$$(m_2)_{(i+1)} = \begin{cases} \max\left\{(1-\xi)(m_2)_{(i)}, 0\right\} & \text{if (i)}, \\ (m_2)_{(i)}\, Q\big((m_2)_{(i)}, \lambda\big)^\eta & \text{if (ii)}, \\ \min\left\{(1+\xi)(m_2)_{(i)}, 1\right\} & \text{if (iii)}, \end{cases} \tag{57}$$

where $\eta$, $\xi$ are real number parameters of the iterative procedure and $(m_2)_{(i)}$, $(m_2)_{(i+1)}$ are the values of $m_2$ for iteration $i$ and $i+1$, respectively. The conditions (i)–(iii) are as follows:

$$\text{(i):} \quad (m_2)_{(i)}\, Q\big((m_2)_{(i)}, \lambda\big)^\eta \leq \max\left\{(1-\xi)(m_2)_{(i)}, 0\right\}, \tag{58}$$

$$\text{(ii):} \quad \max\left\{(1-\xi)(m_2)_{(i)}, 0\right\} \leq (m_2)_{(i)}\, Q\big((m_2)_{(i)}, \lambda\big)^\eta \leq \min\left\{(1+\xi)(m_2)_{(i)}, 1\right\}, \tag{59}$$

$$\text{(iii):} \quad \min\left\{(1+\xi)(m_2)_{(i)}, 1\right\} \leq (m_2)_{(i)}\, Q\big((m_2)_{(i)}, \lambda\big)^\eta, \tag{60}$$

The value of the multiplier $\lambda$ is such that $(m_2)_{(i+1)}$ satisfy the isoperimetric condition (33b). Hence to update $m_2$ it is necessary to solve, with respect to $\lambda$, the following nonlinear equation,

$$\int_\Omega (m_2)_{i+1}(\lambda)\, \mathrm{d}\Omega = A_0. \tag{61}$$

The presented formula is applied for the algorithm whose main steps are:

1. Set the initial $(m_2)_{(0)}$ satisfying the isoperimetric condition (33b); assume the algorithm parameters $\eta$, $\xi$.
2. Solve the equilibrium problem (32) for valid $(m_2)_{(i)}$.
3. Check the stop condition, for instance

$$\frac{C\left((m_2)_{i-1}\right) - C\left((m_2)_i\right)}{C\left((m_2)_{i-1}\right)} < \varepsilon, \tag{62}$$

where $\varepsilon$ is an initially assumed algorithm precision parameter. If the condition is satisfied, then stop, otherwise continue.

4. Using the solution from Step 2 compute

$$\frac{\partial W\left(\boldsymbol{\kappa}(w)_i\,,\,(m_2)_i\right)}{\partial m_2}$$

(appearing in definition (56)).

5. Solve Eq. (61) and according to Eq. (57) update $m_2$ to $(m_2)_{(i+1)}$. Return to Step 2.

The equilibrium problem in Step 2 can be solved using a nonlinear FEM. We have applied this approach successfully for solving examples presented in the consecutive section. To formulate the nonlinear FEM problem the constitutive relation (27) is transformed to the incremental form

$$\mathrm{d}M^{\alpha\beta} = \widehat{D}^{\alpha\beta\lambda\mu}(\boldsymbol{\kappa}, m_2)\mathrm{d}\kappa_{\lambda\mu}\,, \tag{63}$$

where

$$\widehat{D}^{\alpha\beta\lambda\mu}(\boldsymbol{\kappa}, m_2) = D^{\alpha\beta\lambda\mu}(\boldsymbol{\kappa}, m_2) + \frac{\partial D^{\alpha\beta\gamma\eta}(\boldsymbol{\kappa}, m_2)}{\partial \kappa_{\lambda\mu}}\kappa_{\gamma\eta} \tag{64}$$

is so called tangent stiffness moduli tensor [14, 15]. The quantity

$$\frac{\partial D^{\alpha\beta\gamma\eta}(\boldsymbol{\kappa}, m_2)}{\partial \kappa_{\lambda\mu}}\kappa_{\gamma\eta}$$

is nonzero only for regions, where $I(\boldsymbol{\kappa}) \neq 0$ and $\zeta_\kappa \in [\breve{\zeta}_2\,,\,\breve{\zeta}_1]$. In such case it can be expressed as follows,

$$\begin{aligned}\frac{\partial D^{\alpha\beta\gamma\eta}}{\partial \kappa_{\lambda\mu}}\kappa_{\gamma\eta} = -2\breve{A}_\alpha\breve{\zeta}_\alpha\left(\zeta_\kappa\frac{1}{2}\,\delta^{\alpha\beta}\delta^{\lambda\mu} + \frac{1}{\zeta_\kappa}\frac{1}{(II(\boldsymbol{\kappa}))^2}\,I_2^{\alpha\beta\gamma\eta}\kappa_{\gamma\eta}I_2^{\lambda\mu\theta\vartheta}\kappa_{\theta\vartheta}\right)\\ + \sqrt{2}\breve{A}_\alpha\breve{\zeta}_\alpha\frac{I(\boldsymbol{\kappa})}{|I(\boldsymbol{\kappa})|}\,\frac{1}{II(\boldsymbol{\kappa})}\left(\delta^{\alpha\beta}I_2^{\lambda\mu\theta\vartheta}\kappa_{\theta\vartheta} + I_2^{\alpha\beta\gamma\eta}\kappa_{\gamma\eta}\delta^{\lambda\mu}\right).\end{aligned} \tag{65}$$

Referring to the expression (56) it can be seen that the considered updating procedure requires computation of the derivative of potential $W$ with respect to $m_2$. This derivative reads

$$\frac{\partial W}{\partial m_2} = \begin{cases}(I(\boldsymbol{\kappa}))^2\,\dfrac{\partial F(\zeta_\kappa)}{\partial m_2} & \text{if } I(\boldsymbol{\kappa}) \neq 0,\\ \Delta\mu(II(\boldsymbol{\kappa}))^2 & \text{if } I(\boldsymbol{\kappa}) = 0.\end{cases} \tag{66}$$

where

$$\frac{\partial F(\zeta_\kappa)}{\partial m_2} = \begin{cases}\dfrac{\partial \breve{a}_2}{\partial m_2} + \dfrac{\partial \breve{c}_2}{\partial m_2}\,\zeta_\kappa^2 & \text{if } \zeta_\kappa \in \left[0, \breve{\zeta}_2\right],\\ \dfrac{\partial \breve{a}_1}{\partial m_2} + \dfrac{\partial \breve{c}_1}{\partial m_2}\,\zeta_\kappa^2 - \dfrac{\partial \breve{A}_1}{\partial m_2}\left(\zeta_\kappa - \breve{\zeta}_1\right)^2 & \text{if } \zeta_\kappa \in \left[\breve{\zeta}_2\,,\,\breve{\zeta}_1\right],\\ \dfrac{\partial \breve{a}_1}{\partial m_2} + \dfrac{\partial \breve{c}_1}{\partial m_2}\,\zeta_\kappa^2 & \text{if } \zeta_\kappa \geq \breve{\zeta}_1\,.\end{cases} \tag{67}$$

## 5. Circular and annular two-phase plates

We introduce the polar coordinate system $(r, \vartheta)$. We consider annular plates for which $R_i \leq r \leq R_e$, and circular plates when $0 \leq r \leq R$, subjected to rotationally symmetric transverse loading $q = q(r)$. The finite element method is applied. The discretization is performed along the radius; the shape functions are the commonly accepted third order polynomials.

Given are: the radius $R$ or the radii $R_i$, $R_e$, the loading $q$, Young's modulus $E$, Poisson's ratio $\nu$, thicknesses $h_1$, $h_2$ and the volume $V_0$. Let $V = h_2|\Omega|$ be the volume of the plate of constant thickness $h_2$ and given middle plane. Let us define the volume ratio $\gamma = V_0/V$. By Eq. (33b) this ratio is expressed by the formula

$$\gamma = \frac{h_1}{h_2}(1-\beta) + \beta, \tag{68}$$

where $\beta = \frac{A_0}{|\Omega|}$ represents the area ratio. The non-dimensional moments are introduced by the following formulae: $\widetilde{M}_r = M_r/qR^2$, $\widetilde{M}_\vartheta = M_\vartheta/qR^2$. They will be presented in Figs. 3–8; for the sake of simplicity in the notation the tilde over $M$ will be omitted.

### 5.1. Clamped circular plates of a given volume ratio $\gamma$ and $h_1 \geq 0$

We consider a clamped circular two-phase plate of radius $R$, subjected to a uniform loading of intensity $q$. The plate is endowed with the microstructure described in Section 2. The main unknown is the field $m_2 = m_2(r)$, $0 \leq r \leq R$ representing the area fraction of the thickness $h = h_2$. The case of $m_2 = 1$ means that the plate has the constant thickness $h = h_2$. The case of $m_2 = 0$ refers to the case of a plate with constant thickness $h = h_1$. The intermediate values of $m_2$, where $0 < m_2 < 1$, refer to the composite plates of microstructures defined by the invariant $\zeta_\kappa$, cf. Eq. (21). Three types of microstructures corresponding to three regimes of $\zeta_\kappa$, see Section 2, can occur. At the centre of the plate one has $M_I = M_{II}$, hence $\zeta_\kappa = 0$, which refers to the regime 3. Thus around the centre of the plate we expect appearance of the 3rd regime. This regime should have an interface with the 2nd regime (called also the sliding regime).

Let us consider the cases of $\gamma = 0.3$ (Fig. 3a,b,c), $\gamma = 0.5$ (Fig. 3d,e,f), $\gamma = 0.7$ (Fig. 4a,b,c), $\gamma = 0.9$ (Fig. 4d,e,f) for which the distributions of $m_2$, the radial moment $M_r$ and the circumferential moment $M_\vartheta$ are shown as functions of $r/R$ for the subsequent values of the ratio $h_1/h_2$. This ratio varies in the interval $[0, \gamma)$.

We note that around the centre of the plates the 3rd regime prevails. It is shaded in light-grey. For greater $r$ this regime transforms into the sliding regime (shaded in grey), which means that a second rank ribbed plate becomes a first rank ribbed plate. In this (2nd) regime the ribs are directed along the radii. For the extreme case of $h_1/h_2 = 0$ in these regions the plate is incapable of resisting the circumferential bending. In fact, we note that for $h_1/h_2 = 0$ we have $M_\vartheta = 0$ in the 2nd regime, see Figs. 3c, 3f, 4c. The sliding regime usually transforms into the regime 1 of an oblique microstructure, shaded in dark-grey in the figures. Let us remind that this interpretation of the microstructure concerns the case of $h_1 > 0$ but the passage to the limit $(h_1 \to 0)$ looks smooth. Considering greater values of $r$ we note that this regime changes smoothly into the sliding regime (grey shading) and for smaller ratios of $h_1/h_2$ this regime transforms into the 3rd regime (light-grey), see e.g. Fig. 4d.

Depending on the values of $\gamma$ and $h_1/h_2$ the quantity $m_2$ assumes the maximal value 1 around the centre of the plate or, also along the supported edge. If $h_1/h_2 = 0$ the quantity $m_2$ attains the zero value only at one point (defining a circumference) which can be interpreted as a hinge. In other cases, when $h_1/h_2$ does not vanish, $m_2$ can be zero along some intervals (see Fig. 4a,d) which means that there $h = h_1$.

Let us note that the shapes of $M_r$ are quite stable with respect to the $h_1/h_2$ ratio. In contrast, the shapes of plots of $M_\vartheta$ change essentially, when $h_1/h_2$ vary, see e.g. Fig. 4c. These changes are

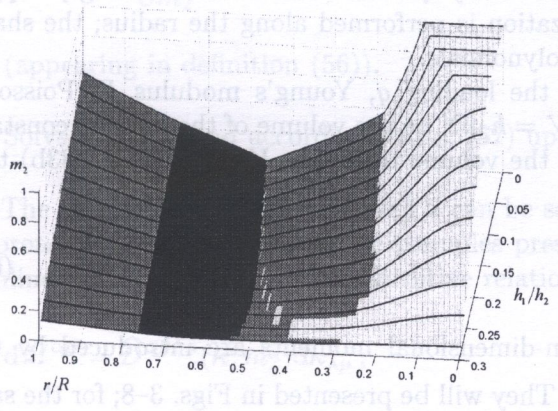


a)

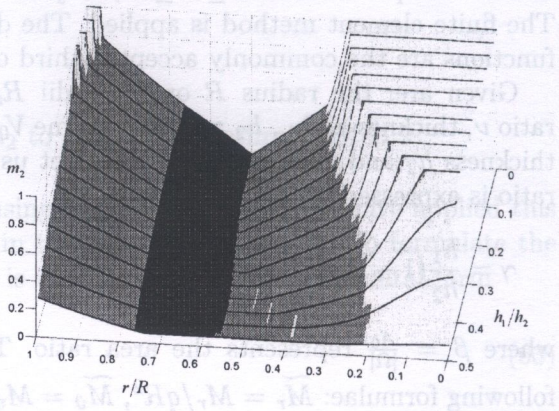


d)

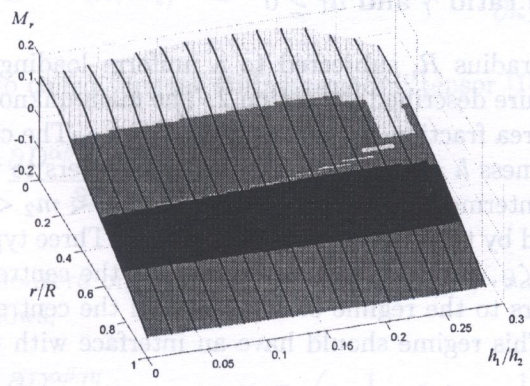


b)

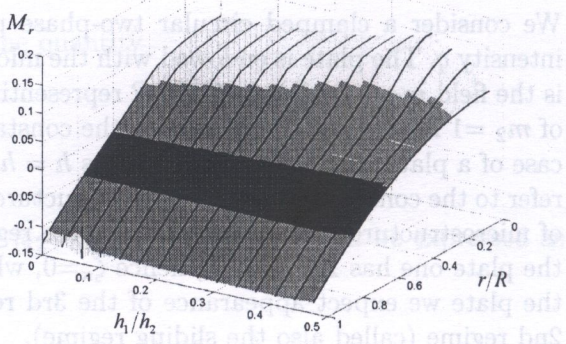


e)

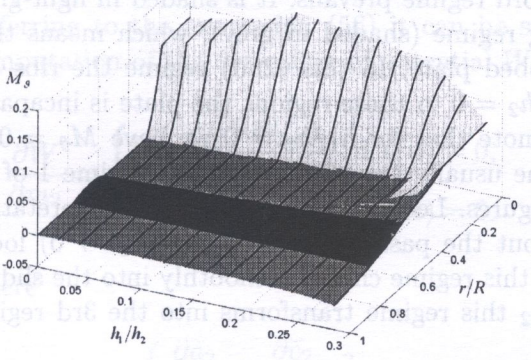


c)

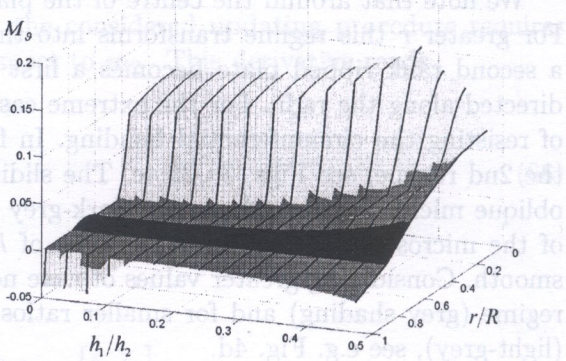


f)

**Fig. 3.** Plots of $m_2(r)$, $M_r(r)$, $M_\vartheta(r)$ in the optimally designed clamped circular plates characterized by different ratios $h_1/h_2 \geq 0$. Case of $\gamma = 0.3$ (a, b, c) and $\gamma = 0.5$ (d, e, f). The loading is uniform

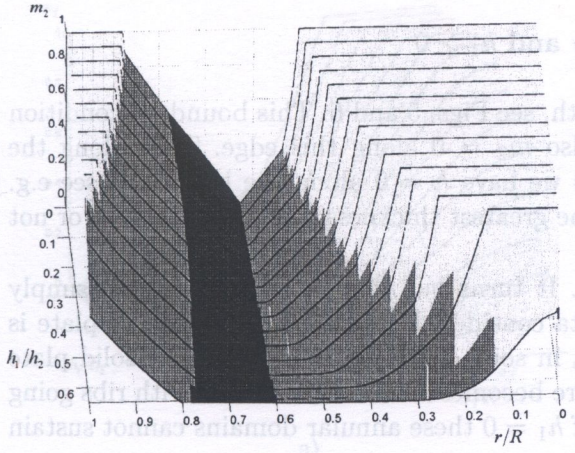


a)

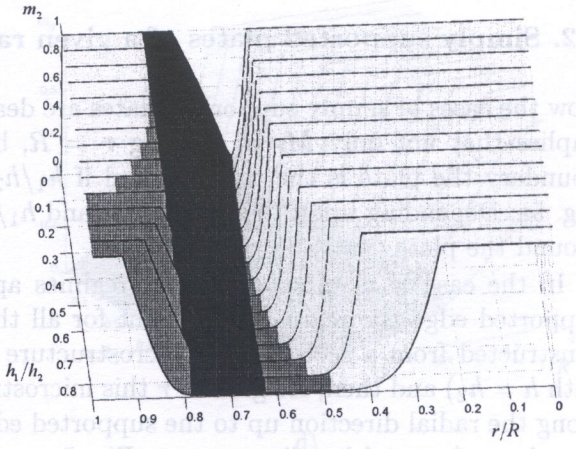


d)

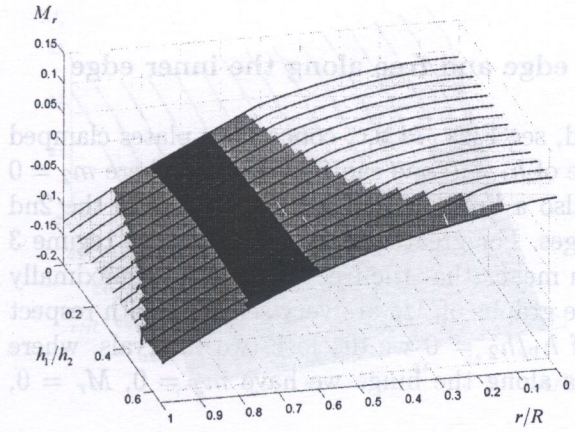


b)

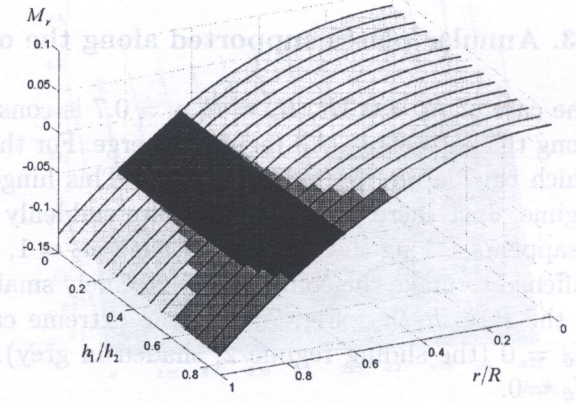


e)

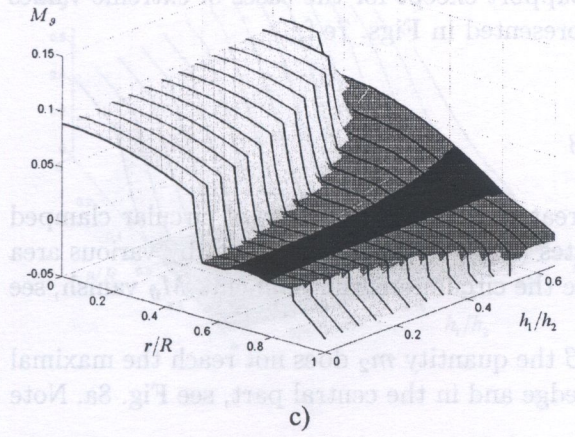


c)

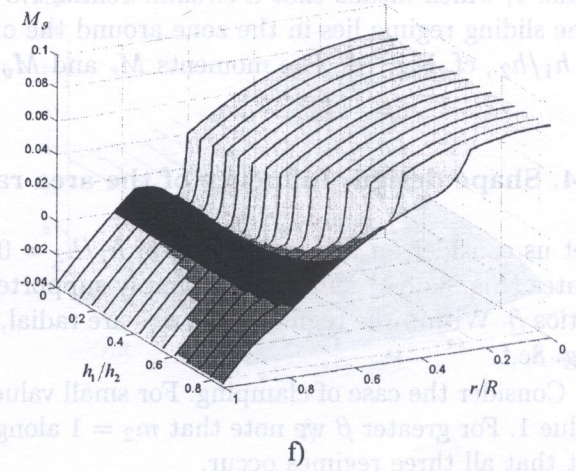


f)

**Fig. 4.** Continuation of Fig. 3 for $\gamma = 0.7$ (a, b, c) and $\gamma = 0.9$ (d, e, f)

linked with that the 2nd rank ribbed plate is quite stiff, but if this microstructure becomes of 1st rank it loses its stiffness rapidly.

### 5.2. Simply supported plates of a given ratio $\gamma$ and $h_1 \geq 0$

Now the cases of simply supported plates are dealt with, see Figs. 5 and 6. This boundary condition implies that not only $M_r = 0$ along $r = R$, but also $m_2 = 0$ along this edge. Thus along the boundary the plate is the thinnest and if $h_1/h_2 = 0$ we have $h = 0$ along the boundary, see e.g. Fig. 5a. Depending upon the values of $\gamma$ and $h_1/h_2$ the greatest thickness $h = h_2$ is achieved or not around the plate centre.

In the case of clamped plates all regimes appear. It turns out that in the case of the simply supported edge the regime 1 is absent for all the data considered. Thus the centre of the plate is constructed from a second rank microstructure (that in some cases degenerates to the solid plate with $h = h_2$) and then, for greater $r$ this microstructure becomes ribbed of first rank with ribs going along the radial direction up to the supported edge. If $h_1 = 0$ these annular domains cannot sustain any circumferential bending, see e.g. Fig. 5c.

### 5.3. Annular plates supported along the outer edge and free along the inner edge

The case of $R_i = 0.3R$, $R_e = R$, $\gamma = 0.7$ is considered, see Figs. 7a,b,c, concerning plates clamped along the outer edge. All regimes emerge. For the case of $h_1 = 0$ one can find a point where $m_2 = 0$ which can be interpreted as a hinge. This hinge is also a line of a jump from the 1st to the 2nd regime. Just there the microstructure suddenly changes. For greater values of $h_1/h_2$ the regime 3 disappears. Along the inner (free) edge $m_2 = 1$, which means that the free edge must be maximally stiffened to make the compliance extremely small. The graphs of $M_\vartheta$ are very sensitive with respect to the ratio $h_1/h_2$, Fig. 7c. For the extreme case of $h_1/h_2 = 0$ we disclose two intervals, where $M_\vartheta = 0$ (the sliding regime 2, shaded in grey). Thus along the hinge we have $m_2 = 0$, $M_r = 0$, $M_\vartheta = 0$.

In the case of simply supported annular plates (with the free inner edge) the variable $m_2$ vanishes along the outer support, while along the inner free boundary this variable reaches its maximal value 1, which means that a circumferential rib occurs, cf. Fig. 7d. The regime 3 does not appear. The sliding regime lies in the zone around the outer support except for the cases of extreme values of $h_1/h_2$, cf. Fig. 7d. The moments $M_r$ and $M_\vartheta$ are presented in Figs. 7e,f.

### 5.4. Shape design. Influence of the area ratio $\beta$

Let us consider an important case of $h_1/h_2 = 0$ in greater detail, for the case of circular clamped plates (Fig. 8a,b,c) and circular simply supported plates (Fig. 8d,e,f) characterized by various area ratios $\beta$. Within the regime 2 the ribs are radial, hence the circumferential moments $M_\vartheta$ vanish, see Fig. 8c,f.

Consider the case of clamping. For small values of $\beta$ the quantity $m_2$ does not reach the maximal value 1. For greater $\beta$ we note that $m_2 = 1$ along the edge and in the central part, see Fig. 8a. Note yet that all three regimes occur.

In the case of simply supported edges only two regimes: 3 and 2 occur, cf. Figs. 8d,e,f. Around the centre $m_2 = 1$ and this region increases together with $\beta$. Along the edge we have $m_2 = 0$ and regime 2 takes place. These results do not coincide with those reported in [25, 26]. The main difference lies in that we disclose the regions, where $m_2 < 1$ and the regime 3 occurs. This means appearance of a 2nd rank ribbed microstructure, absent in all solutions found in [25, 26].

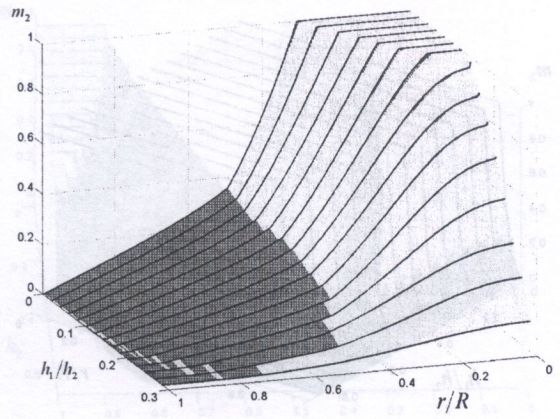


a)

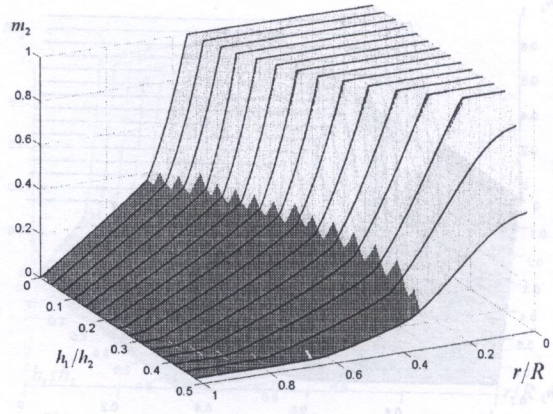


d)

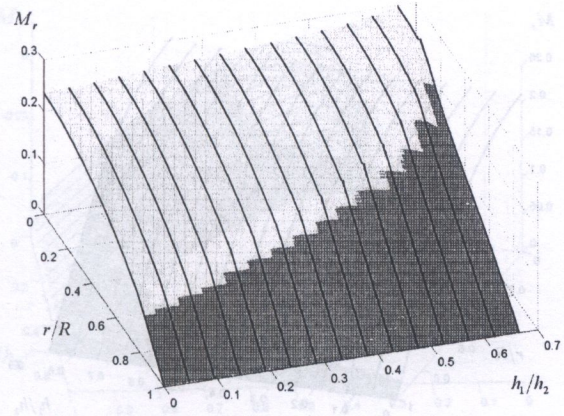


b)

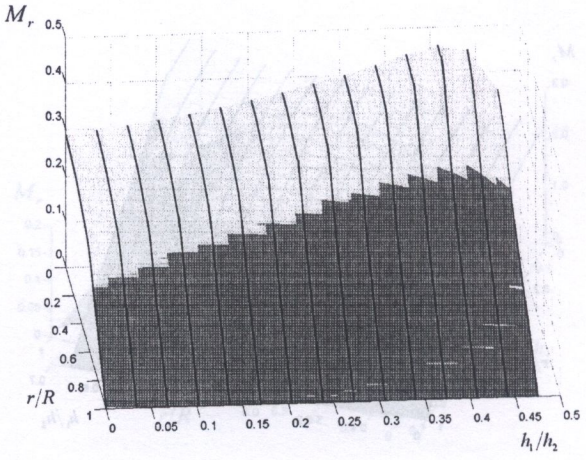


e)

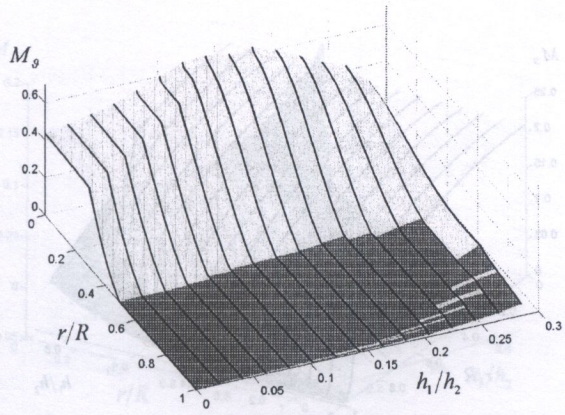


c)

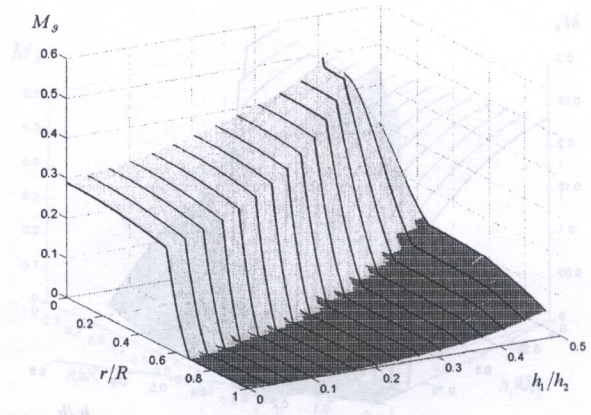


f)

**Fig. 5.** The counterparts of results of Fig. 3 for simply supported plates; $\gamma = 0.3$ (a, b, c) and $\gamma = 0.5$ (d, e, f)

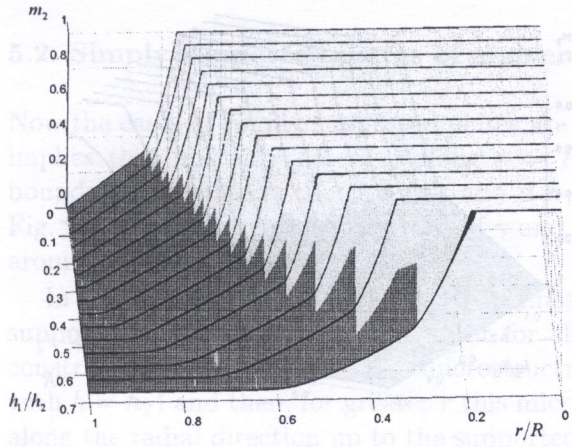


a)

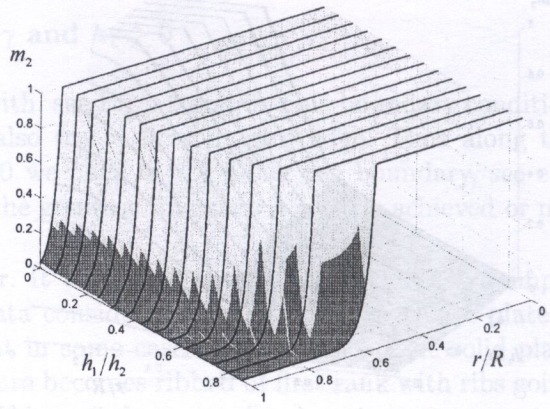


d)

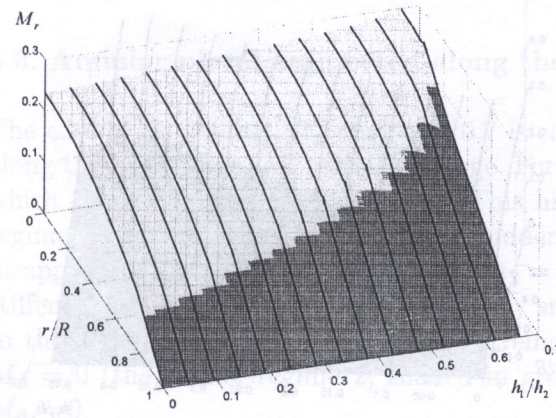


b)

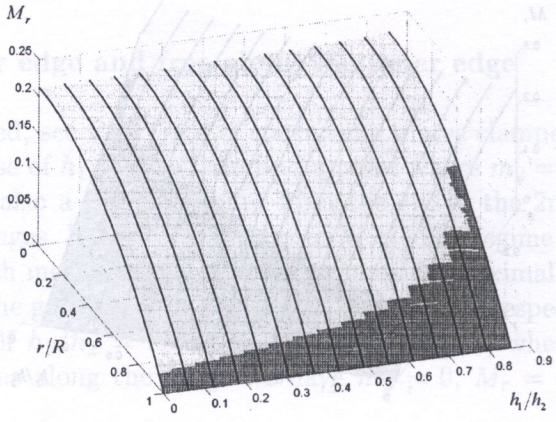


e)

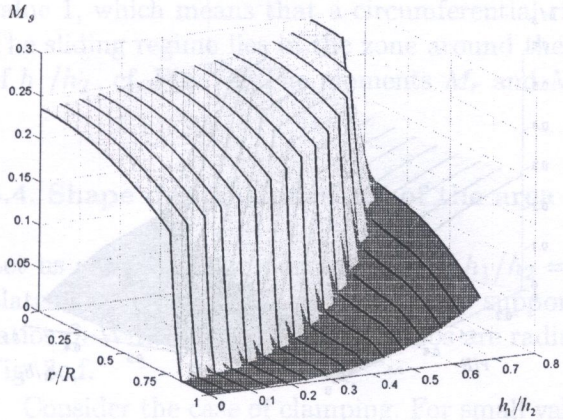


c)

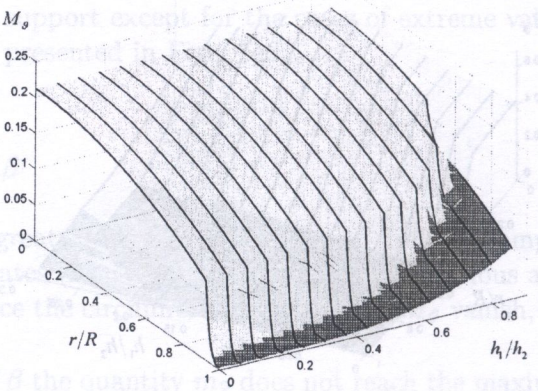


f)

**Fig. 6.** Continuation of Fig. 5 for $\gamma = 0.7$ (a, b, c) and $\gamma = 0.9$ (d, e, f)

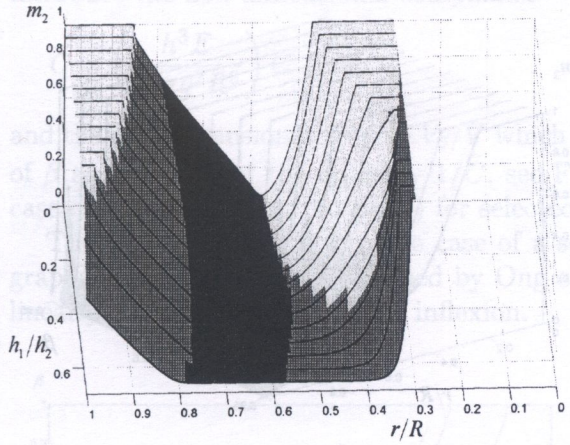


a)

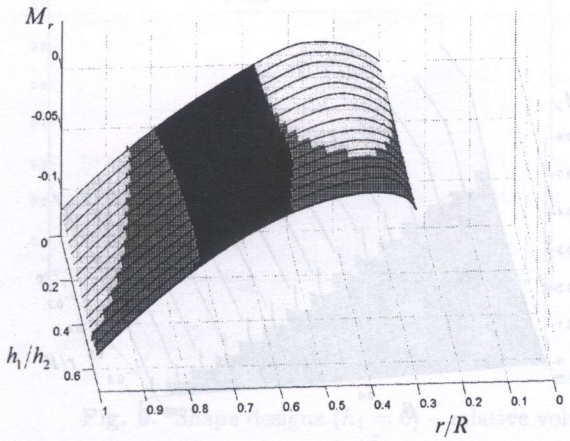


b)

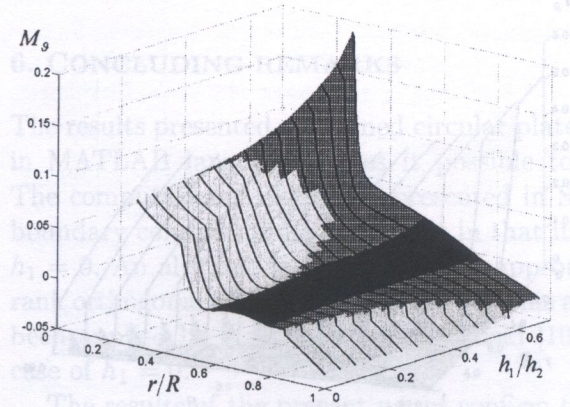


c)

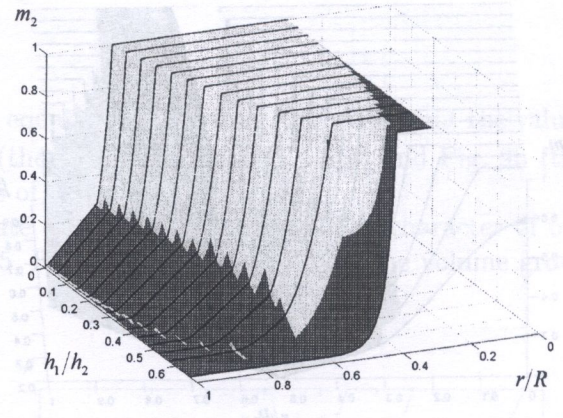


d)

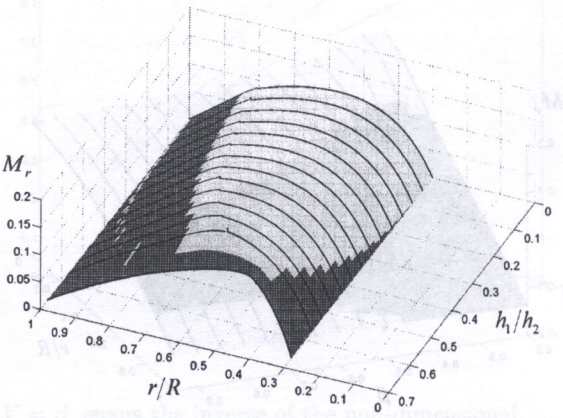


e)

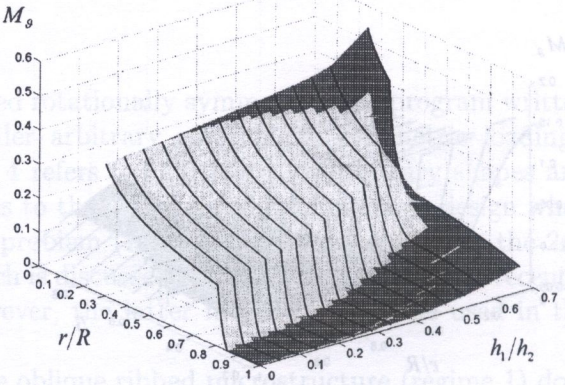


f)

**Fig. 7.** Plots of $m_2(r)$, $M_r(r)$, $M_\vartheta(r)$ in the annular plates; clamped (a, b, c) and simply supported (d, e, f) along the outer boundary. The loading is uniform. Case of $h_1/h_2 \geq 0$ and $\gamma = 0.7$

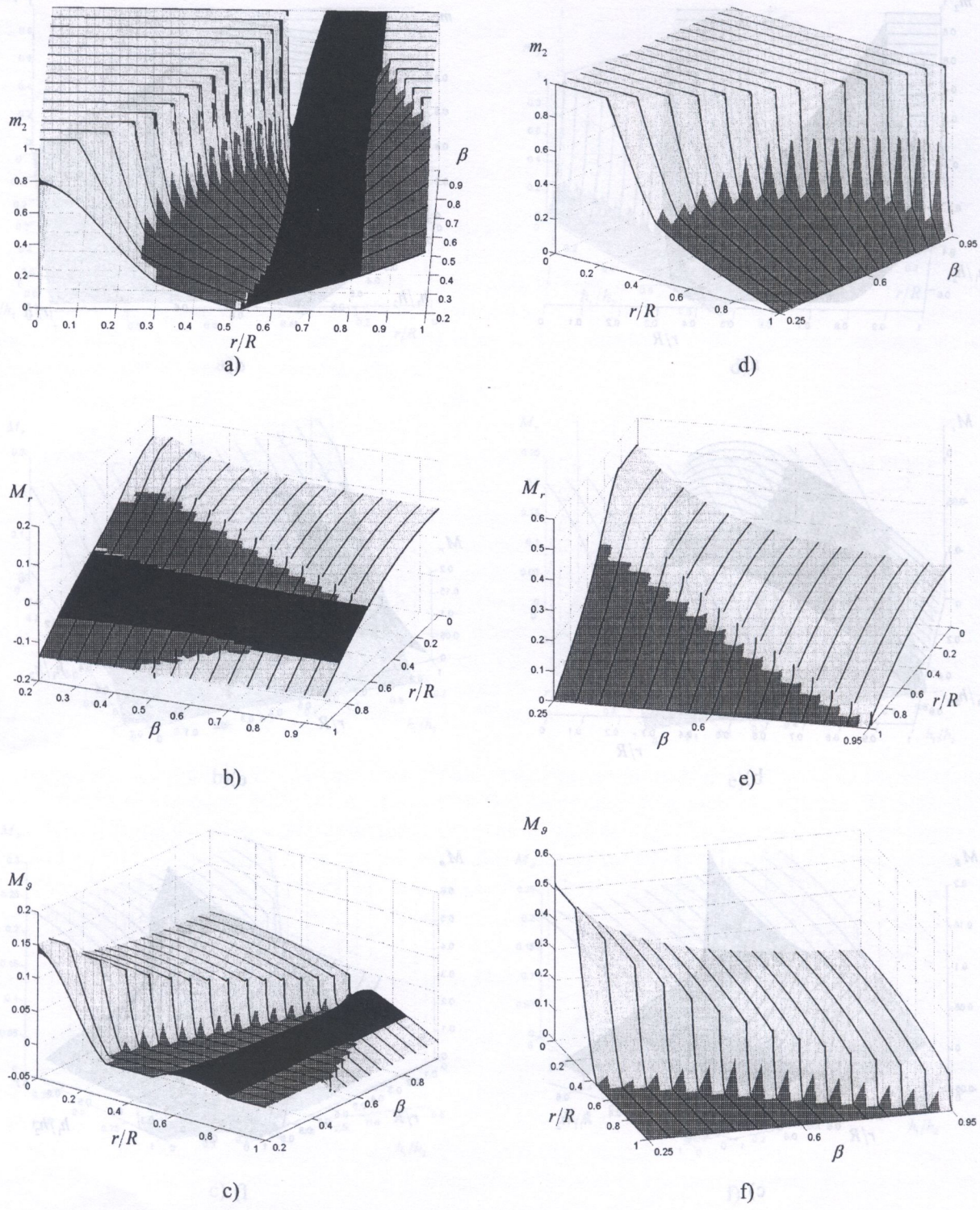


**Fig. 8.** Optimal shape designs (case of $h_1 = 0$) of clamped (a, b, c) and simply supported (d, e, f) circular plates characterized by different ratios $\beta$. The loading is uniform; the Poisson ratio $\nu = 0.2$

### 5.5. Compliance versus the given volume

An optimal plate of a given volume $V_0$ is characterized by its (minimal) compliance $C$. Let us introduce the non-dimensional compliance

$$\widetilde{C} = \left(\frac{h^3 E}{12\pi q^2 R^6}\right) C$$

and the non-dimensional volume $V_0/V$ which is here equal to $\beta$. Following [25] we present the values of $\beta$ as functions of the quantity $1/\widetilde{C}$, see Fig. 9a (the case of a clamped plate) and Fig. 9b (the case of a simply supported plate) for selected values of Poisson's ratio.

The value $\beta = 1$ refers to the case of a solid plate of constant thickness. The character of our graphs is similar to those reported by Ong et al. [25, Figs. 9,11]. For small $1/\widetilde{C}$ the volume grows linearly and then has a point of inflexion.

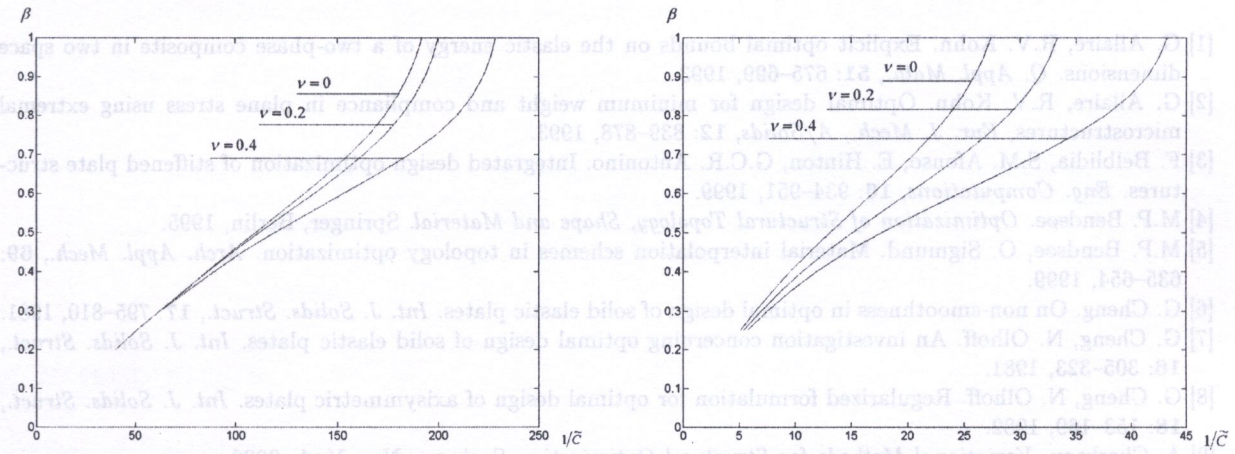


**Fig. 9.** Shape designs ($h_1 = 0$) – relative volume $V_0/V = \beta$ versus the inverse of the non-dimensional compliance $(1/\widetilde{C})$ for the optimal clamped (a) and simply supported (b) plates

## 6. Concluding remarks

The results presented concerned circular plates loaded rotationally symmetric. The program written in MATLAB language makes it possible to consider arbitrary rotationally symmetric loadings. The computational algorithm presented in Section 4 refers to thin plates of arbitrary shapes and boundary conditions. Its virtue lies in that it applies to the degenerated case of shape design when $h_1 = 0$. An alternative computational approach to problem $(P)$ is based upon controlling the 2nd rank orthogonal ribbed microstructure. This approach is discussed by Bendsøe [4, 5] and has recently been applied by Czarnecki and Lewiński [10]. However, the latter method cannot be used in the case of $h_1 = 0$.

The results of the present paper confirm that the oblique ribbed microstructure (regime 1) does appear in the optimal solutions, which has also been observed in [10] in the context of thin two-phase rectangular plates. Note that in the minimum compliance problem for in-plane elasticity this type of microstructure does not appear, see [1, 2, 4, 13, 19]. However, as has been noted by Gibiansky and Cherkaev [13] such oblique microstructures appear in the maximum compliance problem for in-plane elasticity, which reflects a cross-analogy between the minimum compliance problem for Kirchhoff plates and the maximum compliance problem for the 2D elasticity setting, and vice versa, see [19, Sec. 28.4].

The problem of minimum compliance of two-phase plates of moderate thickness has been considered by Díaz et al. [11] in an ingenious manner, by making use of a so-called *moment* formulation. The 3rd rank ribbed microstructures were taken into account. None the less the relaxation formulation for the moderately thick plates is still an open question since the field equations involve length scales thus making the underlying homogenization nonunique, see [19, Sec. 5].

## Acknowledgement

The second author was supported by the Polish Committee for Scientific Research (KBN) through the grant No 7T07A 04318. The computations have been performed by means of the MATLAB system installed in the Computer Centre (COI) of the Warsaw University of Technology.

## References

[1] G. Allaire, R.V. Kohn. Explicit optimal bounds on the elastic energy of a two-phase composite in two space dimensions. *Q. Appl. Math.*, **51**: 675–699, 1993.

[2] G. Allaire, R.V. Kohn. Optimal design for minimum weight and compliance in plane stress using extremal microstructures, *Eur. J. Mech., A/Solids*, **12**: 839–878, 1993.

[3] F. Belblidia, S.M. Afonso, E. Hinton, G.C.R. Antonino. Integrated design optimization of stiffened plate structures. *Eng. Computations*, **16**: 934–951, 1999.

[4] M.P. Bendsøe. *Optimization of Structural Topology, Shape and Material.* Springer, Berlin, 1995.

[5] M.P. Bendsøe, O. Sigmund. Material interpolation schemes in topology optimization. *Arch. Appl. Mech.*, **69**: 635–654, 1999.

[6] G. Cheng. On non-smoothness in optimal design of solid elastic plates. *Int. J. Solids. Struct.*, **17**: 795–810, 1981.

[7] G. Cheng, N. Olhoff. An investigation concerning optimal design of solid elastic plates. *Int. J. Solids. Struct.*, **16**: 305–323, 1981.

[8] G. Cheng, N. Olhoff. Regularized formulation for optimal design of axisymmetric plates. *Int. J. Solids. Struct.*, **18**: 153–169, 1982.

[9] A. Cherkaev, *Variational Methods for Structural Optimization.* Springer, New York, 2000.

[10] S. Czarnecki, T. Lewiński. Optimal layouts of a two-phase isotropic material in thin elastic plates. In: Z. Waszczyszyn, J. Pamin, eds., *Proc. 2nd European Conference on Computational Mechanics, ECCM-2001*, Kraków, 26–29 June 2001. CD-ROM, 2001.

[11] A. Díaz, R. Lipton, C.A. Soto. A new formulation of the problem of optimum reinforcement of Reissner–Mindlin plates. *Comp. Meth. Appl. Mech. Engrg.*, **123**: 121–139. 1995.

[12] H.A. Eschenauer, V.V. Kobelev, A. Schumacher. Bubble method for topology and shape optimization of structures, *Struct. Optimiz.*, **8**: 42–51, 1994.

[13] L.V. Gibiansky, A.V. Cherkaev. Designing composite plates of extremal rigidity (in Russian). Fiziko-Tekhnicheskiy Inst. im. A.F. Ioffe, AN SSSR, preprint No. 914. Leningrad 1984. English translation in: A.V. Cherkaev, R.V. Kohn, eds., *Topics in the Mathematical Modelling of Composite Materials.* Birkhäuser, Boston 1997.

[14] M. Kleiber, C. Woźniak. *Nonlinear Mechanics of Structures.* Polish Scientific Publishers, Warsaw, 1991.

[15] M. Kleiber. Lectures on computer methods in the non-linear thermo-mechanics of deformable bodies (in Polish). Available from `http://www.ippt.gov.pl`, 2001.

[16] R.V. Kohn, G. Strang. Optimal design and relaxation of variational problems. *Comm. Pure Appl. Math.*, **39**: 113–137, 139–183, 353–379, 1986.

[17] K. Kolanek, T. Lewiński, Thin circular plates of minimal compliance. In: W. Szcześniak, ed., *Theoretical Foundations of Civil Engineering*, VII, 316–325. Oficyna Wydawnicza PW, Warszawa 1999.

[18] W. Kozłowski, Z. Mróz. Optimal design of solid plates. *Int. J. Solids. Struct.*, **5**: 781–794, 1969.

[19] T. Lewiński, J.J. Telega. *Plates, Laminates and Shells. Asymptotic Analysis and Homogenization.* World Scientific. Series on Advances in Mathematics for Applied Sciences, vol. 52, Singapore, New Jersey, London, Hong Kong 2000.

[20] T. Lewiński, J.J. Telega. Michell-like grillages and structures with locking, *Arch. Mech.*, **53**: 303–331, 2001.

[21] Q.Q. Liang, Y.M. Xie, G.P. Steven. A performance index for topology and shape optimization of plate bending problems with displacement constraints. *Struct. Multidisc. Optimiz.*, **21**: 393–399, 2001.

[22] R. Lipton. On a saddle-point theorem with application to structural optimization. *J. Optim. Theory. Appl.*, 81: 549–568, 1994.

[23] K.A. Lurie, A.V. Cherkaev. Effective characteristics of composite materials and optimum design of structural members (in Russian). *Adv. Mech. (Uspekhi Mekhaniki)*, **9**: 3–81, 1986.

[24] N. Olhoff, K.A. Lurie, A.V. Cherkaev, A.V. Fedorov. Sliding regimes and anisotropy in optimal design of vibrating axisymmetric plates. *Int. J. Solids. Struct.*, **17**: 931–948, 1981

[25] T.G. Ong, G.I.N. Rozvany, W.T. Szeto. Least-weight design of perforated plates for given compliance: non-zero Poisson's ratio. *Comp. Meth. Appl. Mech. Eng.*, **66**: 301–322, 1988.

[26] G.I.N. Rozvany, N. Olhoff, M.P. Bendsøe, T.G. Ong, R. Sandler, W.T. Szeto. Least-weight design of perforated elastic plates. I,II. *Int. J. Solids. Struct.*, **23**: 521–536, 537–550, 1987.

[27] G.I.N. Rozvany, N. Olhoff, K.-T. Cheng, J.E. Taylor. On the solid plate paradox in structural optimization. *J. Struct. Mech.*, **10**: 1–32, 1982.

[28] L. Tartar. An introduction to the homogenization method in optimal design. In: B. Kawohl, O. Pironneau, L. Tartar, J.-P. Zolesio, eds., *Optimal Shape Design*, 47–156, Springer, Berlin, 2000.

[29] J.J. Telega, T. Lewiński. On a saddle-point theorem in minimum compliance design. *J. Optimiz. Th. Appl.*, **106**: 441–450, 2000.